

Tree-Based Learning in RNNs for Power Consumption Forecasting

Roberto Baviera and Pietro Manzoni, *Politecnico di Milano*

Abstract—A Recurrent Neural Network that operates on several time lags, called an $\text{RNN}(p)$, is the natural generalization of an Autoregressive $\text{ARX}(p)$ model. It is a powerful forecasting tool when different time scales can influence a given phenomenon, as it happens in the energy sector where hourly, daily, weekly and yearly interactions coexist. The cost-effective BPTT is the industry standard as learning algorithm for RNNs. We prove that, when training $\text{RNN}(p)$ models, other learning algorithms turn out to be much more efficient in terms of both time and space complexity. We also introduce a new learning algorithm, the Tree Recombined Recurrent Learning, that leverages on a tree representation of the unrolled network and appears to be even more effective. We present an application of $\text{RNN}(p)$ models for power consumption forecasting on the hourly scale: experimental results demonstrate the efficiency of the proposed algorithm and the excellent predictive accuracy achieved by the selected model both in point and in probabilistic forecasting of the energy consumption.

Index Terms—Recurrent Neural Networks, learning algorithms, complexity estimates, time series forecasting

I. INTRODUCTION

Since the inception of the Recurrent Neural Networks (RNNs), sequence modelling has become a central research topic in deep learning and applications of recurrent architectures have provided excellent results in many different fields [1], [2], [3]. Finding an efficient way for training RNNs, however, has always represented a crucial question for their practical employment with real-world datasets. Backpropagation Through Time [4], hereinafter BPTT, is the most common algorithm used for this purpose. It allows the computation of the gradient of the prediction error with respect to the parameters of the models. Gradient-based algorithms, e.g. Stochastic Gradient Descent (SGD), are then used to calibrate the model on the available data [3].

In the present study, we focus on the use of RNNs for time series forecasting. Properly understanding sequential dependencies in a time series is crucial for making accurate predictions. Standard vanilla RNNs present one feedback loop: they are also called *single-lag* RNNs because they incorporate only a single-lag time delay [3]. A well-known issue with these models is that they often fail in effectively capturing the long-term dependencies. *Multi-lag* RNNs, i.e. networks that incorporate multiple lagged feedbacks, offer an effective solution to this problem: these architectures include shortcuts in the temporal flow of information that allow advanced learning of the existing autocorrelation mechanisms [5]. Different examples of networks with multiple feedbacks can be found in the literature, such as Layered Digital Dynamic Networks (LDDNs), a class of RNNs that is used as the main reference in the MATLAB Deep Learning Toolbox [6], [7].

We consider *shallow* RNNs with multiple Jordan feedbacks [8]. These models appear to be the natural extension of linear Autoregressive models with exogenous inputs, typically denoted in the literature as $\text{ARX}(p)$ models [9]: in the following we will use the compact notation $\text{RNN}(p)$ when referring to these networks.¹ Because they allow explicit feedback connections involving a specific set of lagged outputs, $\text{RNN}(p)$ models can be a powerful forecasting tool when several time scales are involved. Hence, a natural application of these architectures is the forecasting of energy consumption, a relevant socioeconomic variable that exhibits a behavior on different temporal scales (hourly, daily, weekly and yearly) [11].

An important point to underline is that $\text{RNN}(p)$ models offer a clear and intuitive interpretation of their structure. In many industrial applications (as well as in other domains), model explainability is a central requirement: high-stakes decisions necessitate a proper understanding of the predictive models and the currently available methods for explaining deep learning models are often not reliable [12]. In this sense, the black-box approach is not believed to be enough trustworthy and transparent when it comes to making important decisions - for instance, planning the production and the distribution of electricity for an entire country - and to managing the resulting risks. We aim at showing that in our forecasting problem there is no actual trade-off between accuracy and interpretability since $\text{RNN}(p)$ models can even outperform more complex recurrent ones that can be considered only as black-boxes.

In practice, it is well-known that training RNNs can be a difficult task [13]. $\text{RNN}(p)$ models are no exception. As every recurrent model, they require specific learning algorithms for computing the gradient of the loss function with respect to the trainable parameters. Thanks to their structure, this particular class of models can be seen as a special type of Feedforward Neural Networks (FFNNs) that share parameters across time-steps. In the case of shallow vanilla RNNs, i.e. $\text{RNN}(1)$ models, such a feedforward representation is constructed through an ordinary procedure known as the *unrolling* of the Recurrent Neural Network [3], [14]. The standard algorithm used for computing gradients in $\text{RNN}(1)$ models is BPTT [13], [15], which actually is nothing more than the adaptation of the renowned Backpropagation algorithm [16] - originally designed for FFNNs - to an unrolled $\text{RNN}(1)$.

Besides BPTT, another algorithm for gradient computation, named Real-Time Recurrent Learning (RTRL), is also considered in the literature [17]. With RTRL, gradients are computed

¹In the literature, sometimes, expressions such as *NARX* or *recurrent NARX networks* can be found to indicate $\text{RNN}(p)$ models. However, these terms are often used to indicate more general nonlinear models (cf., e.g., [5], [10]).

in real-time as the network runs forward, without needing the explicit storage of the past activity [14]. For RNN(1) models, the computation of leading order of time and space complexity shows that RTRL and BPTT present quite similar complexities, but RTRL can be much more time-consuming than BPTT when the feedback signal is a high dimensional vector [15], [18]. Actually this is not a real issue in the case of univariate time series forecasting because the output of the network is in general a single scalar value.

Nevertheless, there are situations in which BPTT reveals its downsides. We aim at showing that, for RNN(p) models, RTRL can be significantly more time-efficient than BPTT. Backpropagating a gradient can indeed become very onerous in presence of multiple feedbacks. Moreover, the unrolling procedure in presence of a long sequence is in general not efficient: the computational complexity of BPTT scales with the length of the processed sequence and the storage of all intermediate states of the network is required [14].

In the framework of general RNNs with multiple feedbacks, De Jesus and Hagan have first addressed the problem of efficient gradient computation for LDDNs, comparing empirically the training time required by BPTT and RTRL when different network architectures are considered [6]. In the present paper, we compute explicitly the leading order of *time* and *space complexity* for the two algorithms in the RNN(p) framework: we prove that their behaviour is completely different with respect to the RNN(1) case, with RTRL outpacing BPTT. Moreover, we show that every RNN(p) model admits a feed-forward tree representation and, exploiting this equivalence, we identify a new learning algorithm that appears to be extremely efficient.

We conduct the experimental analysis using the GEF-Com2017 dataset [19], which refers to *hourly* households' energy consumption for the New England region (USA). In the energy markets, hourly forecasting is the key temporal resolution for practitioners [20]. Two are the main forecasting techniques: point forecasting and probabilistic forecasting. While in the former RNNs are quite common (see, e.g., [21], [22] and references therein), the literature in the latter case is rather scarce. We adopt a modelling approach similar to the one proposed in [23] for daily forecasting.

The main contributions of the paper are threefold: first, we deduce an explicit formulation for BPTT and RTRL for the considered family of models. In particular, we show that in presence of low-dimensional outputs, RTRL can outperform BPTT in terms of both time and space complexity. Second, taking advantage of the tree representation of RNN(p) models, we propose a novel efficient algorithm, called Tree Recombined Recurrent Learning (TRRL), that is even faster than RTRL. Lastly, we show an application of the presented algorithms to the field of energy consumption forecasting, highlighting how these models can achieve optimal predictive performances.

The rest of the paper is organized as follows. In Section II, we introduce the modelling framework and define the class of RNN(p) models. In Section III, we describe the three algorithms, RTRL, BPTT and TRRL, deducing the time and space complexity associated with their execution. In Section

IV, one application of the considered algorithms is presented. Section V summarizes the results and states our conclusions.

II. MODEL SPECIFICATION: THE RNN(p) CLASS

We consider an RNN with one hidden layer and, as common in regression problems, we assume a linear (i.e. identity) activation function for the output layer [1]. Such a network is specified by the following equations (we adopt the notation used, e.g., in [3] p. 381):

$$\begin{aligned} \mathbf{a}^{(t)} &= \mathbf{b} + U\mathbf{x}^{(t)} + \sum_{i=1}^p W_i \hat{\mathbf{y}}^{(t-i)} \\ \mathbf{h}^{(t)} &= \mathcal{A}(\mathbf{a}^{(t)}) \\ \hat{\mathbf{y}}^{(t)} &= \mathbf{c} + V\mathbf{h}^{(t)}. \end{aligned} \quad (1)$$

We assume the existing feedbacks to be Jordan connections, i.e. output-to-hidden feedbacks [8]. Since the activation function of the output layer is linear, such a network is similar (but not completely equivalent) to an Elman shallow RNN, i.e. with hidden-to-hidden feedbacks [24]. As mentioned in the introduction, the family of models in (1) is the natural nonlinear extension of ARX(p) models, in which previous p outputs are used as inputs for the construction of the next value.

Here, $\mathbf{x}^{(t)} \in \mathbb{R}^x$ denotes the vector of exogenous variables, $\mathbf{h}^{(t)} \in \mathbb{R}^h$ the hidden state and $\hat{\mathbf{y}}^{(t)} \in \mathbb{R}^y$ the output of the model. The kernel matrices U, W_1, \dots, W_p and the bias $\mathbf{b} \in \mathbb{R}^h$ constitute the trainable parameters of the input-to-hidden map. For simplicity of notation, in the following we assume them to be suitably collected in a single vector $\boldsymbol{\theta} \in \mathbb{R}^{(x+py+1)h}$; the size of this vector is denoted as $|\boldsymbol{\theta}|$. An analogous convention applies for V and $\mathbf{c} \in \mathbb{R}^y$: the vector $\boldsymbol{\varphi} \in \mathbb{R}^{(h+1)y}$ collects the weights of the hidden-to-output affine application. We also define for convenience the total number of trainable parameters as

$$w := |\boldsymbol{\theta}| + |\boldsymbol{\varphi}| = (x + py + 1)h + (h + 1)y. \quad (2)$$

In Table I we report the key cardinalities for the considered entities. Finally, we denote by $\mathcal{A} : \mathbb{R}^h \rightarrow \mathbb{R}^h$ any activation function that acts element-wise on the components of the vector $\mathbf{a}^{(t)} \in \mathbb{R}^h$, e.g. a sigmoid activation, and we indicate the loss function as $\mathcal{L} : \mathbb{R}^y \rightarrow \mathbb{R}$, $\mathcal{L} : \hat{\mathbf{y}}^{(t)} \mapsto \ell$.

p	Number of feedback connections
x	Size of exogenous input vector
h	Number of hidden neurons
y	Size of output vector
$ \boldsymbol{\theta} $	Number of input-to-hidden trainable parameters
$ \boldsymbol{\varphi} $	Number of hidden-to-output trainable parameters
w	Total number of trainable parameters
τ	Length of input sequence

TABLE I
NOTATION AND SYMBOLS ADOPTED FOR RNN(p) MODELS.

III. TIME AND SPACE COMPLEXITY IN RNN(p) TRAINING

Standard algorithms used in Neural Networks training are gradient-based [1], [3]. Thus, they require the computation of the gradient of the loss with respect to the trainable weights, which in our framework implies the calculation of the vectors

$$\nabla_{\theta} \mathcal{L} \in \mathbb{R}^{|\theta|} \quad \text{and} \quad \nabla_{\varphi} \mathcal{L} \in \mathbb{R}^{|\varphi|}. \quad (3)$$

Input data for RNNs are sequences: we suppose all the processed sequences to have a fixed length τ . Each input sequence is thus an ordered collection of vectors $\{\mathbf{x}^{(t)}\}_{t=1}^{\tau}$ and we assume to be interested just in the final output $\hat{\mathbf{y}}^{(\tau)}$ (a *many-to-one* approach; see, e.g., [25] and references therein). Thus, the loss associated with each sequence is given by $\mathcal{L}(\hat{\mathbf{y}}^{(\tau)})$.

Gradient computation in Neural Networks is based on the sequential exploitation of the chain rule of derivatives. This happens as a consequence of their peculiar structure, because they are essentially a cascade composition of linear and nonlinear applications. The problem of computing the gradient reduces to a sequence of multiplication of Jacobian matrices and the learning algorithms basically differ in the order in which the multiplications are performed [15].

In the rest of the section, we compute the leading order of time and space complexity of three learning algorithms when applied to RNN(p) models and we compare the obtained results. First, we consider the RTRL, then the BPTT (proving that - in general - its time complexity grows exponentially in τ) and finally a new learning algorithm named Tree Recombined Recurrent Learning (TRRL).

A. Real-Time Recurrent Learning

In the case of RTRL, the computation of the gradients is decomposed as follows:

$$[\nabla_{\theta} \mathcal{L}]^{\top} = [\nabla_{\hat{\mathbf{y}}^{(\tau)}} \mathcal{L}]^{\top} \frac{d\hat{\mathbf{y}}^{(\tau)}}{d\theta} \quad (4a)$$

$$[\nabla_{\varphi} \mathcal{L}]^{\top} = [\nabla_{\hat{\mathbf{y}}^{(\tau)}} \mathcal{L}]^{\top} \frac{d\hat{\mathbf{y}}^{(\tau)}}{d\varphi}. \quad (4b)$$

We denote with $[\cdot]^{\top}$ the transpose operator. The gradient $\nabla_{\hat{\mathbf{y}}^{(\tau)}} \mathcal{L}$, which is a common term in the two equations, can be deduced when the final forecast $\hat{\mathbf{y}}^{(\tau)}$ has been obtained, i.e. when the last exogenous input of the sequence, $\mathbf{x}^{(\tau)}$, has been processed. In addition, for every $t = 1 : \tau$, the following recursive relationships hold:

$$\frac{d\hat{\mathbf{y}}^{(t)}}{d\theta} = V \frac{d\mathbf{h}^{(t)}}{d\mathbf{a}^{(t)}} \left(\frac{\partial \mathbf{a}^{(t)}}{\partial \theta} + \sum_{i=1}^p W_i \frac{d\hat{\mathbf{y}}^{(t-i)}}{d\theta} \right) \quad (5a)$$

$$\frac{d\hat{\mathbf{y}}^{(t)}}{d\varphi} = \frac{\partial \hat{\mathbf{y}}^{(t)}}{\partial \varphi} + V \frac{d\mathbf{h}^{(t)}}{d\mathbf{a}^{(t)}} \sum_{i=1}^p W_i \frac{d\hat{\mathbf{y}}^{(t-i)}}{d\varphi}. \quad (5b)$$

Notice that the inferred output $\hat{\mathbf{y}}^{(t)}$ depends on θ and φ in two different manners. First, a variation in the weights modifies the “instantaneous” relation between the output $\hat{\mathbf{y}}^{(t)}$ and the inputs provided to the RNN at time t (i.e. $\mathbf{x}^{(t)}, \hat{\mathbf{y}}^{(t-1)}, \dots, \hat{\mathbf{y}}^{(t-p)}$); we denote with partial derivatives, e.g. $\partial \hat{\mathbf{y}}^{(t)} / \partial \varphi$, this kind of dependency, that accounts for the feedforward behavior of the model. Second, the recurrent

inputs at time t , i.e. $\hat{\mathbf{y}}^{(t-1)}, \dots, \hat{\mathbf{y}}^{(t-p)}$, are in turn functions of θ and φ because they are previous outputs of the same model. Moreover, it is easy to deduce that $\partial \mathbf{a}^{(t)} / \partial \theta$ is a sparse matrix with just one nonzero entry for every column. This result is intuitive, since every weight corresponds to a single link between two neurons in consecutive layers.

According to RTRL, it is possible to obtain the values at time t of the Jacobian matrices $d\hat{\mathbf{y}}^{(t)} / d\theta \in \mathbb{R}^{y \times |\theta|}$ and $d\hat{\mathbf{y}}^{(t)} / d\varphi \in \mathbb{R}^{y \times |\varphi|}$ as functions of their previous values. (cf. equations (5a) and (5b)). For $t \leq 0$, we assume $\hat{\mathbf{y}}^{(t)} = \mathbf{0}$ and a null initialization of the corresponding Jacobian matrices.

Matrix multiplication is performed left-to-right and, for the chosen activation function, $d\mathbf{h}^{(t)} / d\mathbf{a}^{(t)}$ is a diagonal matrix. The number of operations required by equations (5a) and (5b) is $\mathcal{O}(p y^2 |\theta|)$ and $\mathcal{O}(p y^2 |\varphi|)$, respectively. Thus, the time complexity associated with the processing of the entire sequence of length τ can be estimated as

$$\mathcal{O}(\tau p y^2 w). \quad (6)$$

For what concerns space complexity, the algorithm requires the storage of the last p Jacobian matrices: hence, the actual memory requirement is

$$\mathcal{O}(p y w). \quad (7)$$

B. Backpropagation Through Time

As mentioned, BPTT is the industry standard for vanilla RNNs and its functioning is based on the unrolled representation of an RNN [1], [3]. In detail, the backpropagation procedure works as follows: after having processed the entire sequence, the gradients of the last output with respect to the weights are obtained as

$$[\nabla_{\theta} \mathcal{L}]^{\top} = [\nabla_{\hat{\mathbf{y}}^{(\tau)}} \mathcal{L}]^{\top} V \frac{d\mathbf{h}^{(\tau)}}{d\mathbf{a}^{(\tau)}} \left(\frac{\partial \mathbf{a}^{(\tau)}}{\partial \theta} + \sum_{i=1}^p W_i \frac{d\hat{\mathbf{y}}^{(\tau-i)}}{d\theta} \right) \quad (8a)$$

$$[\nabla_{\varphi} \mathcal{L}]^{\top} = [\nabla_{\hat{\mathbf{y}}^{(\tau)}} \mathcal{L}]^{\top} \left(\frac{\partial \hat{\mathbf{y}}^{(\tau)}}{\partial \varphi} + V \frac{d\mathbf{h}^{(\tau)}}{d\mathbf{a}^{(\tau)}} \sum_{i=1}^p W_i \frac{d\hat{\mathbf{y}}^{(\tau-i)}}{d\varphi} \right). \quad (8b)$$

However, here, the Jacobian matrices $d\hat{\mathbf{y}}^{(\tau-i)} / d\theta$ and $d\hat{\mathbf{y}}^{(\tau-i)} / d\varphi$ are not previously computed and stored as in RTRL, but recursively calculated “unrolling” the RNN backwards-in-time. As the first step, we obtain

$$[\nabla_{\theta} \mathcal{L}]^{\top} = [\nabla_{\hat{\mathbf{y}}^{(\tau)}} \mathcal{L}]^{\top} V \frac{d\mathbf{h}^{(\tau)}}{d\mathbf{a}^{(\tau)}} \left(\frac{\partial \mathbf{a}^{(\tau)}}{\partial \theta} + \sum_{i=1}^p W_i V \frac{d\mathbf{h}^{(\tau-i)}}{d\mathbf{a}^{(\tau-i)}} \left(\frac{\partial \mathbf{a}^{(\tau-i)}}{\partial \theta} + \sum_{j=1}^p W_j \frac{d\hat{\mathbf{y}}^{(\tau-i-j)}}{d\theta} \right) \right) \quad (9a)$$

$$[\nabla_{\varphi} \mathcal{L}]^{\top} = [\nabla_{\hat{\mathbf{y}}^{(\tau)}} \mathcal{L}]^{\top} \left(\frac{\partial \hat{\mathbf{y}}^{(\tau)}}{\partial \varphi} + V \frac{d\mathbf{h}^{(\tau)}}{d\mathbf{a}^{(\tau)}} \sum_{i=1}^p W_i \left(\frac{\partial \hat{\mathbf{y}}^{(\tau-i)}}{\partial \varphi} + V \frac{d\mathbf{h}^{(\tau-i)}}{d\mathbf{a}^{(\tau-i)}} \sum_{j=1}^p W_j \frac{d\hat{\mathbf{y}}^{(\tau-i-j)}}{d\varphi} \right) \right) \quad (9b)$$

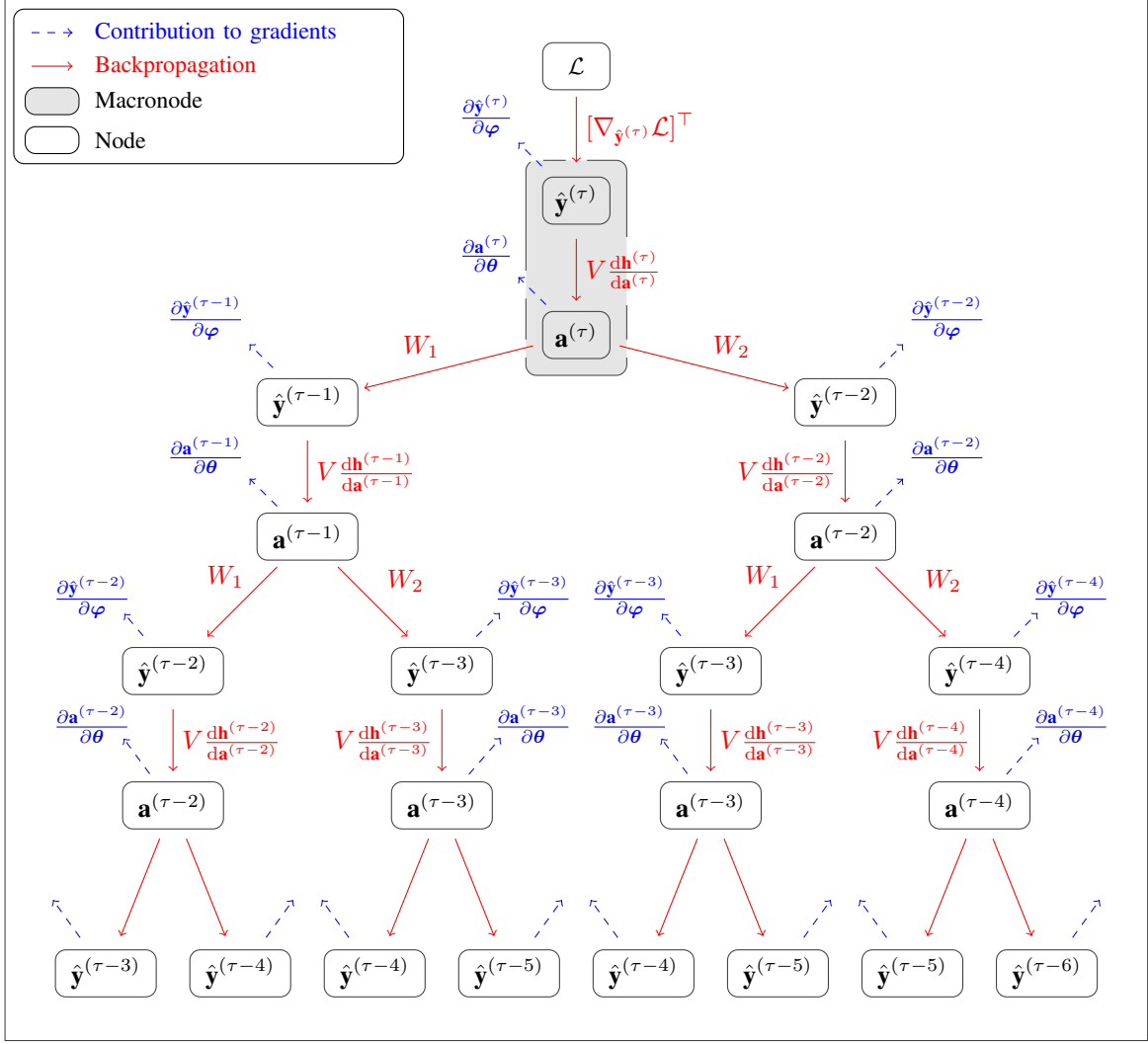


Fig. 1. Computational graph of Backpropagation Through Time for an RNN(2). The unrolling procedure allows the representation of the RNN as a tree: since, for every t , $\mathbf{a}^{(t)}$ is a function of $\hat{\mathbf{y}}^{(t-1)}$ and $\hat{\mathbf{y}}^{(t-2)}$, we obtain this characteristic dichotomous structure. Red solid lines represent the backpropagation flows, while blue dashed lines the contributions of each node to the gradients $\nabla_{\theta}\mathcal{L}$ and $\nabla_{\varphi}\mathcal{L}$. Lastly, we denote with the gray rectangle a macronode, the fundamental unit considered to compute the complexity of this algorithm.

and then we recursively expand the expressions for the Jacobian matrices $d\hat{\mathbf{y}}^{(\tau-i)}/d\theta$ and $d\hat{\mathbf{y}}^{(\tau-i)}/d\varphi$. The advantage of this approach is that, since the product of the matrices is performed from left to right, it actually becomes a chain of matrix-vector multiplications. In the case of RNN(1) models, this trick allows to achieve a significant reduction of the computational effort [15].

In the RNN(p) framework, however, the presence of multiple feedbacks introduces some criticalities in the functioning of the algorithm. Figure 1 shows the computational graph of BPTT in the case of an RNN(2) model, i.e. a network with two lagged feedbacks. For each “macronode”, i.e. for each pair of nodes $(\mathbf{a}^{(t)}, \hat{\mathbf{y}}^{(t)})$ in the graph, the computational effort can be estimated to be $\mathcal{O}(w)$. Thus, the time complexity of BPTT is given by

$$\mathcal{O}(N_{macro} w) \quad (10)$$

being N_{macro} the total number of macronodes in the graph.

It is possible to show that N_{macro} is equal to the sum of the

first τ numbers of a p -bonacci sequence [26] with initial value equal to 1. In particular, for $p = 2$, this quantity coincides with the sum of the first τ numbers of a Fibonacci sequence:

$$\sum_{i=1}^{\tau} F_i = F_{\tau+2} - 1. \quad (11)$$

One can easily prove that the partial sums of p -bonacci grow exponentially in τ . This fact determines the unfeasibility of the BPTT on the graph even for fairly short sequences.

In terms of memory storage, BPTT requires the instantaneous access to all inputs $\{\mathbf{x}^{(t)}\}_{t=1}^{\tau}$, intermediate states $\{\mathbf{a}^{(t)}\}_{t=1}^{\tau}$, hidden states $\{\mathbf{h}^{(t)}\}_{t=1}^{\tau}$ and outputs $\{\hat{\mathbf{y}}^{(t)}\}_{t=1}^{\tau}$. Moreover, the recursive implementation of the algorithm as defined in equations (9a) and (9b) prescribes the storage of a suitable number of intermediate gradients (of size h)²: this number depends on the depth of the computational tree and

²Actually, the RNN(1) case is the only one that does not require storage of the intermediate gradients (see, e.g., [18]).

thus, in the worst case, it is equal to τ . Therefore, the space complexity can be estimated as

$$\mathcal{O}(\tau(x + 3h + y)), \quad (12)$$

a quantity that can become significantly large in presence of long sequences. For many practical cases, we can approximate $(x + 3h + y)$ with w/h . This shows that when the problem requires the analysis of long sequences, in particular when τ is greater than pyh , RTRL outperforms BPTT in terms of both time and space complexity.

C. Tree Recombined Recurrent Learning

In this subsection, we introduce a new algorithm, even faster than RTRL, that leverages on the tree structure of the unrolled RNN(p) models. Let us consider for simplicity the $p = 2$ case, as depicted in Figure 1. If we look at the two subgraphs (one on the main left branch and one on the main right branch) that originate from node $\hat{\mathbf{y}}^{(\tau-2)}$, it is easy to notice that they are identical. This is completely reasonable because the history that brings to the construction of $\hat{\mathbf{y}}^{(\tau-2)}$ is the same in the two cases, but this vector separately contributes to the creation of both $\hat{\mathbf{y}}^{(\tau-1)}$ and $\hat{\mathbf{y}}^{(\tau)}$. The *total* gradient of the loss with respect to $\hat{\mathbf{y}}^{(\tau-2)}$, called \mathbf{g}_2 hereinafter, is given by

$$\begin{aligned} \mathbf{g}_2^\top &:= [\nabla_{\hat{\mathbf{y}}^{(\tau-2)}} \mathcal{L}]^\top = \\ &= [\nabla_{\hat{\mathbf{y}}^{(\tau)}} \mathcal{L}]^\top V \frac{d\mathbf{h}^{(\tau)}}{d\mathbf{a}^{(\tau)}} \left(W_1 V \frac{d\mathbf{h}^{(\tau-1)}}{d\mathbf{a}^{(\tau-1)}} W_1 + W_2 \right). \end{aligned} \quad (13)$$

Analogously, we can define as \mathbf{g}_i the *total* gradient of the loss with respect to $\hat{\mathbf{y}}^{(\tau-i)}$: this gradient accounts for all contributions that $\hat{\mathbf{y}}^{(\tau-i)}$ brings to the construction of the output $\hat{\mathbf{y}}^{(\tau)}$. For instance, \mathbf{g}_1 is simply given by

$$\mathbf{g}_1^\top = V(d\mathbf{h}^{(\tau)}/d\mathbf{a}^{(\tau)}) W_1, \quad (14)$$

while \mathbf{g}_3 can be obtained as

$$\mathbf{g}_3^\top = \mathbf{g}_1^\top V \frac{d\mathbf{h}^{(\tau-1)}}{d\mathbf{a}^{(\tau-1)}} W_2 + \mathbf{g}_2^\top V \frac{d\mathbf{h}^{(\tau-2)}}{d\mathbf{a}^{(\tau-2)}} W_1 \quad (15)$$

By suitably exploiting the \mathbf{g}_i vectors, we can recombine the tree and avoid useless repetitions of the subgraphs. Moreover, $\nabla_{\theta} \mathcal{L}$ and $\nabla_{\varphi} \mathcal{L}$ can be expressed as

$$\begin{aligned} \top &= \sum_{i=0}^{\tau} \mathbf{g}_i^\top V \frac{d\mathbf{h}^{(\tau-i)}}{d\mathbf{a}^{(\tau-i)}} \frac{\partial \mathbf{a}^{(\tau-i)}}{\partial \theta} \\ [\nabla_{\varphi} \mathcal{L}]^\top &= \sum_{i=0}^{\tau} \mathbf{g}_i^\top \frac{\partial \hat{\mathbf{y}}^{(\tau-i)}}{\partial \varphi}. \end{aligned} \quad (16)$$

In a general RNN(p) model, the vectors $\{\mathbf{g}_i\}_{i=0}^{\tau-1}$ can be constructed through Algorithm 1. We can estimate its time complexity as

$$\mathcal{O}(\tau w), \quad (17)$$

since the leading terms are again the multiplications that involve the sparse matrices $\partial \mathbf{a}^{(\tau-i)}/\partial \theta$ and $\partial \hat{\mathbf{y}}^{(\tau-i)}/\partial \varphi$. Space complexity is instead analogous to the one of BPTT. The only difference is that, at the i -th iteration of the outer loop, only the vectors $\mathbf{g}_i, \dots, \mathbf{g}_{i+p}$ have to be stored.

Algorithm 1 Tree Recombined Recurrent Learning (TRRL)

```

 $\mathbf{g}_0 \leftarrow \nabla_{\hat{\mathbf{y}}^{(\tau)}} \mathcal{L}$ 
for  $i = 0 : \tau - 1$  do
   $\nabla_{\varphi} \mathcal{L} += [\frac{\partial \hat{\mathbf{y}}^{(\tau-i)}}{\partial \varphi}]^\top \mathbf{g}_i$ 
   $\mathbf{g}_i \leftarrow [V \frac{d\mathbf{h}^{(\tau-i)}}{d\mathbf{a}^{(\tau-i)}}]^\top \mathbf{g}_i$ 
   $\nabla_{\theta} \mathcal{L} += [\frac{\partial \mathbf{a}^{(\tau-i)}}{\partial \theta}]^\top \mathbf{g}_i$ 
  for  $l = 1 : p$  do
    if  $i + l < \tau$  then
       $\mathbf{g}_{i+l} += W_l^\top \mathbf{g}_i$ 
    end if
  end for
  delete  $\mathbf{g}_i$ 
end for

```

We call the algorithm Tree Recombined Recurrent Learning (TRRL) because it inherits the best properties of BPTT and RTRL, which are - respectively - the gradient propagation on the unrolled tree and a time complexity which is linear in τ .³

Table II summarizes the computational properties of the analyzed algorithms in terms of time complexity and space complexity.

	Time Complexity	Space Complexity
TRRL	$\mathcal{O}(\tau w)$	$\mathcal{O}(\tau(x + 2h + py))$
RTRL	$\mathcal{O}(\tau p y^2 w)$	$\mathcal{O}(p y w)$
BPTT	$\mathcal{O}(N_{macro}(\tau) w)$	$\mathcal{O}(\tau(x + 3h + y))$

TABLE II
TIME COMPLEXITY AND SPACE COMPLEXITY FOR THE CONSIDERED ALGORITHMS. AS DISCUSSED IN SECTION III-B, $N_{macro}(\tau)$ IS RELATED TO A p -BONACCI SEQUENCE, THUS IT GROWS EXPONENTIALLY IN τ .

IV. RNN(p) FOR POWER CONSUMPTION FORECASTING

In this section, we compare the computational and predictive performances achieved by RNN(p) models. We consider a relevant problem in the energy sector, that is the forecasting of electricity consumption. We test our models on a real-world dataset, used for the Global Energy Forecasting Competition (GEFCom) in 2017 [19]. It contains the aggregated households' hourly consumption in MWh for the New England region (USA), together with averaged wet-bulb and dry-bulb hourly temperatures in Fahrenheit degrees. Data are published by the overseer of the New England bulk electric power system, ISO New England (ISONE).

We aim at forecasting the future hourly electricity consumption on a one-year-ahead time horizon, a problem that in the literature is known as *mid-term* forecasting [27]. Depending on the considered time horizon, the dynamics of

³Moreover, we emphasize that TRRL works not only when all previous p lags are provided to the network, but also in the case in which some of them are missing (e.g. if we select some specific lags that we believe to be relevant for the model, as in a general linear AR model).

energy consumption appear to be affected by different factors, e.g. climatic, demographic and economic ones. In particular, weather conditions are renowned to be the main driver in mid-term forecasting [28]. As standard in the field [27], [29], we aim to produce *ex-post* forecasts, i.e. to predict the future consumption considering realized weather as known.

We consider, in the following, two main forecasting paradigms: point forecasting and probabilistic forecasting. The former is aimed at producing predictions in the form of scalar values, that is, to predict the exact value of power consumption at a given hour t . The latter is instead aimed at generating predictions in the form of probability distributions. Usual machine learning models for time series forecasting do not rely on hypothesis on the distribution of the noise (like whiteness or Gaussianity, as linear stationary models do [9]) and therefore point forecasts cannot convey any detail about the uncertainty associated with each prediction.

For this reason, the goal of probabilistic forecasting is to offer a stochastic description of each forecast, providing details about confidence and variability. This aspect is very important in the energy sector because, for instance, power utility companies need to accurately plan the production and the distribution of electricity [27]. The knowledge of the confidence intervals of each prediction is crucial to quantify, on the one hand, the risk of overloading the distribution grid and, on the other one, the overproduction of energy [29].

In the following, we describe our modelling methodology, highlighting the relevance of $\text{RNN}(p)$ models and how they can be used both in point and in probabilistic forecasting. Then we illustrate and comment on the obtained results: in evaluating the performances we analyze two main indicators, forecasting accuracy and computational efficiency.

A. Methodology

For the experimental analysis, we consider the consumption data for the period 2007-2014. As shown in Figure 2, we initially split our time series into a training set (2007-2010), a validation set (2011) and a test set (2012). The remaining years are used to check the robustness of our forecasting procedure.

The methodology consists of three steps: first, we detrend and deseasonalize the time series of electrical consumption; second, we use an $\text{RNN}(p)$ model to process the residual signal; finally, we assemble the *ex-post* forecasts by aggregating

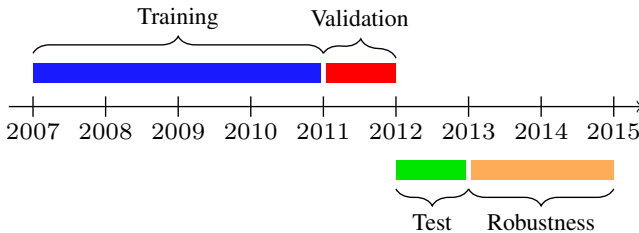


Fig. 2. Dataset segmentation. Models are initially trained on the 2007-2010 data and the grid search procedure is performed considering 2011 as validation set. The best hyperparameters are then selected and a second training is performed on the 2008-2011 data, using the year 2012 as test set. The remaining years of data are finally utilized for robustness checks.

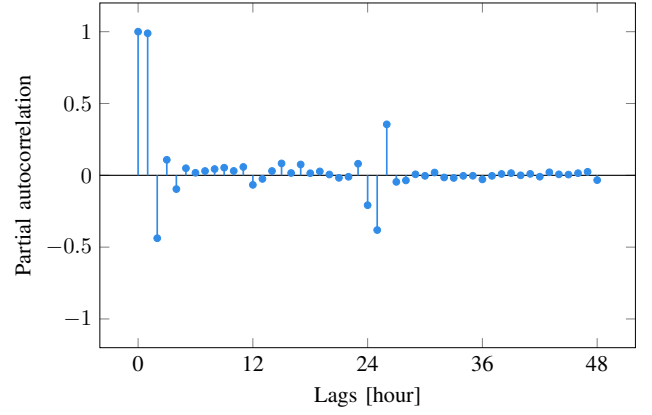


Fig. 3. Autocorrelation structure of in-sample residuals (2007-2010). The PACF highlights the presence of a peculiar serial correlation: lags 1 and 2 are identified to be extremely relevant, as well as the ones around lag 24.

the seasonal forecasts and the $\text{RNN}(p)$ forecasts. As standard in the energy sector, we consider as regressand variable the (normalized) logarithm of the consumption (see, e.g., [30] and references therein).

1) *Deseasonalization*: The removal of the macroscopical seasonal behavior is a standard operation in time series analysis. It is aimed at achieving the stationarity of the time series and it is proven to increase the learning ability of a Neural Network [31], [32]. We perform this initial operation by using a General Linear Model (GLM), which is calibrated through Ordinary Least Squares (OLS). In particular, we process separately each of the 24 hours of the day and, at this stage, only calendar variables are used as regressors.

2) *Analysis of the residual time series*: The residuals of the linear regression are then studied employing an $\text{RNN}(p)$ model. The selection of recurrent lags is performed by exploiting the Partial Autocorrelation Function (PACF), commonly used to identify the relevant autoregressive dependencies in a time series [9]. In the case of electricity consumption, the time series appears to have a very strong and distinctive autocorrelation. Figure 3 shows the PACF diagram of in-sample residuals. It is possible to identify two distinct autoregressive mechanisms: they involve respectively an hourly dependency (the consumption during the very last hours before) and a daily dependency (what has happened around 24 hours before).

Both in case of point and probabilistic forecasting, we split the original dataset into overlapping sequences with length equal to two days: as underlined by the PACF diagram, the pieces of information contained in the previous 48 hours are relevant to generate a reliable forecast. Thus, our training set is composed of 35063 sequences with $\tau = 49$ and each element of a sequence is a vector containing some calendar variables and the two available temperatures. In particular, we use a sinusoidal encoding for the hour-of-the-day and the day-of-the-year, a dummy encoding for the day-of-the-week and an additional dummy variable to identify holidays.

The difference between point and probabilistic forecasting lies in the choice of the loss function. For point forecasting, we select MSE as objective function to be minimized during training, a choice which is rather common in the literature of

load forecasting with Neural Networks [21], [33]. For what concerns probabilistic forecasting, we adopt the modelling approach proposed by Azzone and Baviera [23] for the daily case, but focusing on hourly consumption. We model the consumption for the hour t as a lognormal random variable and we train the $\text{RNN}(p)$ to predict the mean μ_t and the standard deviation σ_t of each density. Every output is a bidimensional vector ($y = 2$) and - during the training - we aim at maximizing the Gaussian loglikelihood over the sample. In other words, the quantity

$$-\frac{1}{N} \sum_{t=1}^N \log \left(\frac{1}{\sqrt{2\pi}\sigma_t} \exp \left\{ -\frac{1}{2} \left(\frac{r_t - \mu_t}{\sigma_t} \right)^2 \right\} \right)$$

is used as loss function for training, where r_t is the residual of the GLM and N the size of the mini-batch. Finally, we choose to use a sigmoid activation function for the hidden layer.

3) *Aggregation of forecasts*: When the training of the Neural Network is completed, we generate one year of predictions of hourly power consumption. Actually, the $\text{RNN}(p)$ model generates predictions for the residual signal - the one obtained after the removal of the seasonal behaviour. This is the most interesting component of our forecasts, since the Neural Network is expected to capture the complex relationship between power consumption and weather conditions. To obtain the final predictions, we also need to generate the forecasts for the seasonal part using the GLM introduced in subsection IV-A1.

In the case of point forecasting, the final forecast is given by the sum of the two forecasts, the one of GLM and the one of $\text{RNN}(p)$. In the probabilistic case, each GLM forecast acts as a shift for the mean of the Gaussian density generated by the Neural Network. According to our methodology, the (normalized) logarithm of the consumption at time t , denoted by C_t , is thus predicted as

$$C_t \sim \mathcal{N}(s_t + \mu_t, \sigma_t^2),$$

being s_t the GLM seasonal forecast at time t . As the last step, the obtained forecasts are denormalized and exponentiated.

For our analysis we use a lookahead of 1 year, i.e. we produce *ex-post* hourly forecasts for an entire year. We stress that realized power consumption of the validation/test set is not progressively made available: the model just learns how to optimally exploit its own previous forecasts to generate future forecasts.

A validation phase is conducted to choose the best hyperparameters for $\text{RNN}(p)$ models (the linear models, instead, do not require any hyperparameter selection). We identify

Hyperparameter	Values
Hidden Neurons	5, 10, 15
Learning Rate	1e-4, 5e-4, 1e-3
Batch Size	32, 64

TABLE III

SET OF HYPERPARAMETERS ANALYZED IN THE GRID SEARCH FOR BOTH POINT AND PROBABILISTIC FORECASTING.

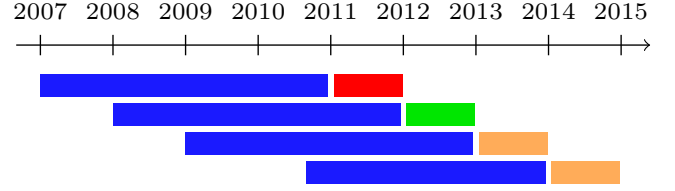


Fig. 4. Scheme of the walk-forward approach. The length of the training set is kept fixed (equal to 4 years) and a rolling-window methodology is adopted.

three possible neural architectures: as suggested by the PACF diagram in Figure 3, we select $\{1\}$, $\{1, 2\}$ and $\{1, 2, 24\}$ as sets of autoregressive lags to be used as Jordan feedbacks. Hence, in the first case we have a vanilla RNN, while in the other cases two different $\text{RNN}(p)$ models. In the next section, we compare the results obtained using the three architectures. This ablation study is intended to quantify the impact of adding specific feedback connections and to help the interpretability of the model.

For each of the three Neural Networks, we perform a grid search on the set of values reported in Table III. We investigate in particular three critical hyperparameters: two are associated with the training procedure (namely, the learning rate and the batch size) and the other one (the number of hidden neurons) with the structure of the network. We use Adam [34] as optimizer and the training is stopped if no increment on the loss is observed for 100 epochs.

B. Forecasting accuracy

In this section, we discuss the results obtained on the test set (2012) and on the two following years. We adopt a *walk-forward testing* approach [35], as schematized in Figure 4. In particular, we always keep the length of the training set equal to 4 years. This choice is motivated by two main reasons. First, the worldwide electricity demand is rapidly changing: consumption needs in modern society require an ever-increasing amount of electricity, as a consequence of the improvements in the standard of living and of the economic expansion. Second, changes in the energy sector are in general disruptive: a time horizon too far in the past is likely to describe a situation significantly different from the one we desire to forecast [36].

We assess the accuracy of the point forecast by means of Root Mean Square Error (RMSE) and Mean Absolute Percentage Error (MAPE). Table IV reports the results of the testing phase on the year 2012. As shown, the inclusion of the second and the twenty-fourth lag brings a relevant benefit in terms of model predictive performances. The increase in forecasting precision on the test set is around 8% in relative terms. Furthermore, we obtain extremely accurate point forecasts; MAPE is indeed significantly below 2.5%: according to practitioners, this is the threshold that identifies a very good model for *ex-post* forecasting.

Similar predictive performances are observed in the probabilistic framework. In this case, we evaluate the accuracy on the test set by considering RMSE and MAPE (of the expected value of each distribution), and we also compute the Average

RNN(p)	RMSE [MWh]	MAPE [%]
{1}	447.62	2.27
{1, 2}	436.60	2.15
{1, 2, 24}	421.05	2.09

TABLE IV
RESULTS OF POINT FORECASTING ON THE TEST SET (2012).

Pinball Loss (APL), a standard measure of density forecasting error [27]. Table V summarizes the results on the test set, considering again the three different feedback architectures. Not only multi-lag RNNs obtain a better point accuracy, but also the predicted densities are more appropriate to describe the distributions of the future consumption, as highlighted by APL. Figure 5 shows the probabilistic forecasts in two periods of the year, the first weeks of March and August, which are characterized by completely different weather conditions. Results are impressive: the point forecast accurately reproduces the behaviour of realised consumption throughout the entire period. Moreover, in all cases, the realised consumption falls within the 95% confidence intervals (CI).

In Table VI, we provide the accuracy results obtained with two benchmark models: an ARX model with the same set of autoregressive explicatory variables as the best performing RNN (i.e. using the forecasts 1h, 2h and 24h before) and an LSTM network⁴. It is possible to notice that the RNN(p) outperforms both benchmark models. On the one hand, ARX generates rather poor forecasts, on the other, the optimally selected RNN appears to be more accurate even than the LSTM, the recurrent architecture considered the state-of-the-art in time series forecasting.

Moreover, in probabilistic forecasting is crucial to *backtest* the CIs, counting the fraction of hours the realised power consumption falls within a confidence level α of the predicted density and comparing it to the theoretical level. Let us emphasize that LSTM probabilistic forecasts show a worse backtesting performance of several percentage points compared to RNN(p) for all α in the range 90% – 99%.

Furthermore, as standard in econometrics, we also check the robustness of our approach by considering two additional test years, 2013 and 2014. Table VI collects RMSE and MAPE for these robustness tests in the probabilistic case. The results highlight how multi-lag RNN(p) are capable of bringing a significant improvement in the accuracy metrics: the measured improvements of RNN({1, 2, 24}) with respect to RNN(1) are reported to be up to 14% in absolute terms and 15% in relative terms.

Finally, it is important to underline that not only RNN(p) models are able to generate extremely accurate forecasts, but they do so without sacrificing simplicity and interpretability.

Analogous results are found in the case of point forecasting.

⁴In the LSTM case, the model has been trained using the same methodology described above - including the validation phase - considering a shallow Neural Network with an LSTM hidden layer.

RNN(p)	RMSE [MWh]	MAPE [%]	APL [MWh]
{1}	451.18	2.26	117.03
{1, 2}	435.58	2.17	113.45
{1, 2, 24}	417.83	2.02	106.09

TABLE V
RESULTS OF PROBABILISTIC FORECASTING ON THE TEST SET (2012).

C. Algorithmic Efficiency

We evaluate the computational efficiency by measuring the average time which is required for each epoch of the training.⁵ Figure 6 shows the observed training time for the three learning algorithms in the point forecasting case for different values of τ ; we consider here an RNN(2), thus, we take $\tau = 3$ as the minimum sequence length. As expected, the computational effort required by BPTT grows exponentially in τ : this fact entails the practical impossibility of capturing daily dependencies for BPTT and the need for finding alternative efficient algorithms. Instead, the time complexity associated with TRRL and RTRL grows linearly in τ , in accordance with the complexity estimates in Section III.

A second experimental analysis that we propose concerns the computational efficiency as a function of the number of recurrent connections (i.e. the order p of the model) and hidden neurons. Table VII collects the measured time-per-epoch for training a multi-lag RNN in the probabilistic case; analogous empirical results are found for point forecasting. Notice that time-per-epoch in the case of BPTT is not reported for the unfeasibility of the algorithm (except in the case $p = 1$, when BPTT actually coincides with TRRL). Even in this case, TRRL proves to be much more efficient than RTRL, in particular when a substantial number of neurons is considered. We observe that the former algorithm is faster than the latter by a factor which is close to the theoretical value $4p$. Moreover, let us emphasize that these measurements include the time required for the forward propagation procedure and the impact of lower-order terms, which are neglected in our complexity estimate.

V. CONCLUSIONS

In this paper, we have analyzed under a theoretical and an empirical perspective three different learning algorithms that can be used for training a family of shallow RNNs with Jordan feedbacks, called the RNN(p) models. These models are the natural nonlinear extension of the well-known ARX(p) models: for this reason, they are characterized by extreme versatility and by a high level of interpretability. We have focused on how to efficiently compute the gradient of the loss function with respect to the parameters of the network in presence of multi-lag recurrent connections and we have proposed an application of these models in a relevant real-world problem.

⁵Neural Networks have been trained on *gigat*, the computational cluster of MOX (Politecnico di Milano), using MPI parallelization (8 parallel processes running on a machine with 5 nodes, 20 Intel Xeon E5-2640 and 384GB RAM).

We have shown that not only the proposed $\text{RNN}(p)$ model is as simple to be interpreted as a standard $\text{ARX}(p)$ model, but it allows to achieve higher accuracy with respect to an LSTM network, the state-of-the-art in time series forecasting.

The main contributions of this paper are threefold. First, we have shown that the standard implementation of BPTT reveals to be not efficient when dealing with $\text{RNN}(p)$ models. We have analytically estimated the leading order of complexity of BPTT on the computational graph: it grows exponentially with respect to the length of the processed sequence, implying *de facto* the unfeasibility of the algorithm in most cases. This family of models is a clear example where RTRL, the main alternative to BPTT according to the literature, works better than BPTT as learning algorithm: on the one hand, it is not affected by any exponential growth in time complexity; on the other, when networks are limited in size, RTRL is in general more efficient than BPTT also in terms of space complexity.

Second, we have introduced a novel algorithm for gradient computation that can be applied to the considered family of recurrent networks. It is called Tree Recombined Recurrent Learning and is based on a tree representation of the unrolled RNN. In detail, it allows smart recombination of the branches of the computational tree, leading to a huge reduction in the time required for training.

Lastly, we have presented the application of the proposed models and algorithms in a forecasting problem that is central in the energy sector. It represents an example in which considering long sequences is necessary in order to properly capture relevant features of the analyzed phenomenon. We have evaluated the performances in terms of computational time and forecasting accuracy: we have shown that $\text{RNN}(p)$ models are able to produce high-precision forecasts at the hourly scale in terms of both point and probabilistic forecasting. Finally, in line with the complexity estimates of Section III, TRRL is recognized to be the most efficient learning algorithm.

ACKNOWLEDGMENTS

We are grateful for valuable insights and assistance from M. Roveri and A. Falcetta (Politecnico di Milano, Dept. of Electronics, Information and Bioengineering). We would like to thank M. Azzone, C. Alasseur, Y. Goude, A. Stizia and T. Serafin for helpful suggestions and all participants to the conferences “Big Data and Machine Learning in Finance” (Milan) and “EFI7” (Naples). A special thank goes to the members of the OSIRIS department in EDF R&D (Paris) and to all attendees at the EDF seminar “ $\text{RNN}(p)$ for Power

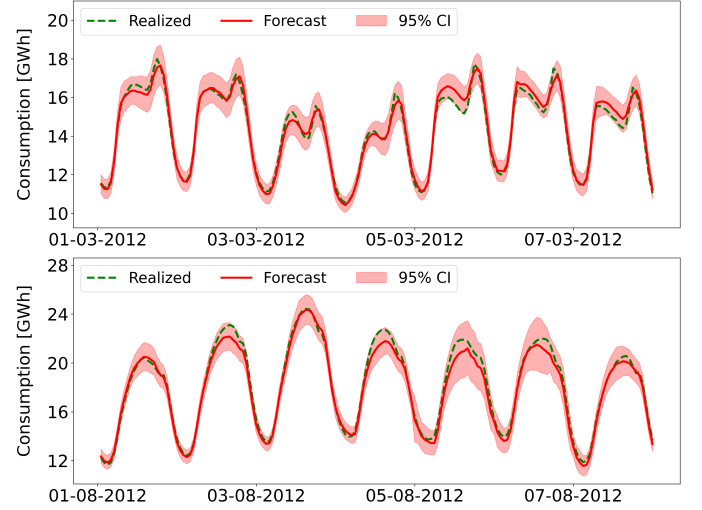


Fig. 5. Density forecasts of hourly power consumption on the test set (2012). Realised (dashed green line) and expected (red line) power consumption in GWh for the first week of March and August, respectively. The shaded area represents the 95% confidence interval for each prediction. The forecasts capture effectively the intra-daily behavior of the electrical load during every hour of the day and, in terms of density, realised consumption falls within the 95% CI in all cases. Plotted predictions are the ones produced by the $\text{RNN}(\{1, 2, 24\})$.

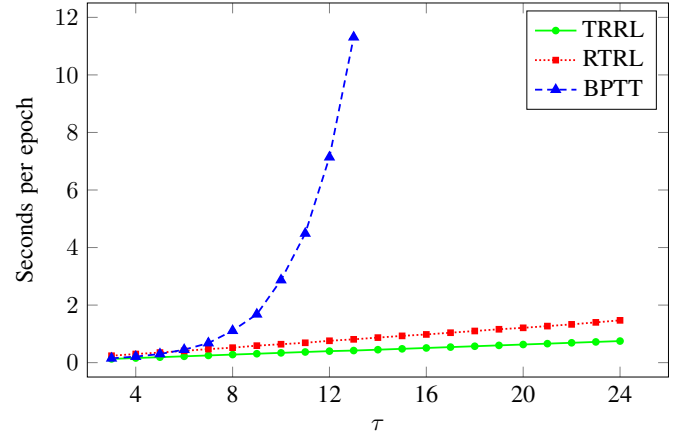


Fig. 6. Observed training time (in seconds per epoch) against sequence length τ for the three algorithms. We consider an RNN for point forecasting ($y = 1$) with 15 Hidden Neurons and two autoregressive feedbacks ($p = 2$). TRRL and BPTT have similar behavior when τ is very small ($\tau \leq 4$): in this case, they are both faster than RTRL. However, when we process long sequences, the time-per-epoch grows exponentially for BPTT, as a consequence of the Fibonacci term; instead, the growth is linear for TRRL and RTRL.

Year	Probabilistic Forecasting							
	RMSE [MWh]				MAPE [%]			
	ARX	LSTM	RNN(1)	RNN($\{1, 2, 24\}$)	ARX	LSTM	RNN(1)	RNN($\{1, 2, 24\}$)
2012	1092.05	485.21	451.18	417.83	5.96	2.49	2.26	2.02
2013	1204.40	433.86	419.60	397.51	6.31	2.08	2.15	2.04
2014	1016.86	491.65	442.17	382.55	6.27	2.60	2.30	1.94

TABLE VI

COMPARISON WITH ARX AND LSTM: RESULTS ON THE TEST SET AND ROBUSTNESS CHECKS FOR THE PROBABILISTIC FORECASTING.

	TRRL [sec/ep]			RTRL [sec/ep]			Gain
Neurons	5	10	15	5	10	15	factor
{1}	0.57	1.07	1.66	1.49	2.80	4.14	4
{1, 2}	0.67	1.19	1.82	2.70	5.32	7.91	8
{1, 2, 24}	0.71	1.28	1.93	4.31	8.97	13.12	12

TABLE VII

TIME-PER-EPOCH REQUIRED BY LEARNING ALGORITHMS AS A FUNCTION OF THE NUMBER OF HIDDEN NEURONS, WHEN PERFORMING A TRAINING IN THE PROBABILISTIC FRAMEWORK ($\tau = 49$). WE OBSERVE THAT FOR TRRL THE COMPUTATIONAL TIME DOES NOT DEPEND ON THE ORDER p OF THE RNN, WHILE THE GAIN FACTOR OF TRRL WITH RESPECT TO RTRL IS APPROXIMATELY EQUAL TO THE THEORETICAL ONE, INDICATED IN THE LAST COLUMN.

Consumption Forecasting” for stimulating questions and comments.

REFERENCES

- [1] C.C. Aggarwal, *Neural Networks and Deep Learning. A textbook*, Springer, 2016.
- [2] A. Graves, *Supervised Sequence Labelling with Recurrent Neural Networks*, Springer, 2012.
- [3] I. Goodfellow, Y. Bengio and A. Courville, *Deep Learning*, MIT Press, 2016.
- [4] P.J. Werbos, “Backpropagation through time: what it does and how to do it,” in *Proceedings of the IEEE*, vol. 78, no. 10, pp. 1550–1560, 1990.
- [5] T. Lin, B.G. Horne, P. Tino and C.L. Giles, “Learning long-term dependencies in NARX recurrent neural networks,” *IEEE Transactions on Neural Networks*, vol. 7, no. 6, pp. 1329–1338, 1996.
- [6] O. De Jesus and M.T. Hagan, “Backpropagation Algorithms for a Broad Class of Dynamic Networks,” *IEEE Transactions on Neural Networks*, vol. 18, no. 1, pp. 14–27, 2007.
- [7] M.H. Beale, M.T. Hagan and H.B. Demuth, “Deep Learning Toolbox - User’s Guide,” The Mathworks Inc., 2022.
- [8] M.I. Jordan, “Attractor Dynamics and Parallelism in a Connectionist Sequential Machine,” in *The Eighth Annual Conference of the Cognitive Science Society, Amherst, MA, US*, pp. 531–546, 1986.
- [9] G.E. Box, G.M. Jenkins, G.C. Reinsel and G.M. Ljung, *Time series analysis: forecasting and control*, Fifth edition, John Wiley & Sons, 2015.
- [10] S. Billings, *Nonlinear System Identification: NARMAX Methods in the Time, Frequency, and Spatio-Temporal Domains*, John Wiley & Sons, 2013.
- [11] T. Hong, *Short Term Electric Load Forecasting*, Ph.D. Thesis, North Carolina State University, Charlotte, NC, US, 2010.
- [12] C. Rudin, “Stop explaining black box machine learning models for high stakes decisions and use interpretable models instead,” *Nature Machine Intelligence*, vol. 1, pp. 206–215, 2019.
- [13] R. Pascanu, T. Mikolov and Y. Bengio, “On the difficulty of training recurrent neural networks,” in *JMLR Workshop and Conference Proceedings, ICML(3)*, vol. 28, pp. 1310–1318, 2013.
- [14] O. Marshall, K. Cho and C. Savin, “A unified framework of online learning algorithms for training recurrent neural networks,” *Journal of Machine Learning Research*, vol. 21, pp. 1–34, 2020.
- [15] R.J. Williams and D. Zipser, “Gradient-based learning algorithms for recurrent networks and their computational complexity,” in Y. Chauvin and D.E. Rumelhart (Eds.), *Backpropagation: Theory, architectures, and applications*, pp. 433–486, Lawrence Erlbaum Associates Inc., 1995.
- [16] D.E. Rumelhart, G.E. Hinton and R.J. Williams “Learning representations by back-propagating errors,” *Nature*, vol. 323, pp. 533–536, 1986.
- [17] R.J. Williams and D. Zipser, “A Learning Algorithm for Continually Running Fully Recurrent Neural Networks,” *Neural Computation*, vol. 1, no. 2, pp. 270–280, 1989.
- [18] J. Menick, E. Elsen, U. Evci, S. Osindero, K. Simonyan and A. Graves, “A Practical Sparse Approximation for Real Time Recurrent Learning,” *arXiv preprint arXiv:2006.07232*, 2020.
- [19] T. Hong, J. Xie and J. Black, “Global energy forecasting competition 2017: Hierarchical probabilistic load forecasting,” *International Journal of Forecasting*, vol. 35, no. 4, pp. 1389–1399, 2019.
- [20] N. Elamin and M. Fukushima, “Modeling and forecasting hourly electricity demand by SARIMAX with interactions,” *Energy*, vol. 165, pp. 257–268, 2018.
- [21] F.M. Bianchi, E. Maiorino, M.C. Kampffmeyer, A. Rizzi and R. Jenssen, *Recurrent Neural Networks for Short-Term Load Forecasting - An Overview and Comparative Analysis*, Springer, 2017.
- [22] L.C.M. de Andrade, M. Oleskovicz, A.Q. Santos and D.V. Coury and R.A. Souza Fernandes, “Very short-term load forecasting based on NARX recurrent neural networks,” in *2014 IEEE PES General Meeting*, pp. 1–5, 2014.
- [23] M. Azzone and R. Baviera, “Neural network middle-term probabilistic forecasting of daily power consumption,” *Journal of Energy Markets*, vol. 1, no. 14, pp. 1–26, 2021.
- [24] J.L. Elman, “Finding Structure in Time,” *Cognitive Science*, vol. 14, no. 2, pp. 179–211, 1990.
- [25] Z.C. Lipton, J. Berkowitz and C. Elkan, “A Critical Review of Recurrent Neural Networks for Sequence Learning,” *arXiv preprint arXiv:1506.00019*, 2015.
- [26] D.A. Wolfram, “Solving generalized Fibonacci recurrences,” *Fibonacci Quarterly*, vol. 36, no. 2, pp. 129–145, 1998.
- [27] T. Hong and S. Fan “Probabilistic electric load forecasting: A tutorial review,” *International Journal of Forecasting*, vol. 32, no. 3, pp. 914–938, 2016.
- [28] R.J. Hyndman and S. Fan, “Density Forecasting for Long-Term Peak Electricity Demand,” *IEEE Transactions on Power Systems*, vol. 25, pp. 1142–1153, 2010.
- [29] S. Fan and R.J. Hyndman, “Short-Term Load Forecasting Based on a Semi-Parametric Additive Model,” *IEEE Transactions on Power Systems*, vol. 27, pp. 134–141, 2012.
- [30] J. Nowotarski and R. Weron, “Recent advances in electricity price forecasting: A review of probabilistic forecasting,” *Renewable and Sustainable Energy Reviews*, vol. 81, pp. 1548–1568, 2018.
- [31] G.P. Zhang and M. Qi, “Neural network forecasting for seasonal and trend time series,” *European Journal of Operational Research*, vol. 160, no. 2, pp. 501–514, 2005.
- [32] M. Nelson, T. Hill, W. Remus and M. O’Connor, “Time series forecasting using neural networks: should the data be deseasonalized first?,” *Journal of Forecasting*, vol. 18, pp. 359–367, 1999.
- [33] E. Machado, T. Pinto, V. Guedes and H. Morais, “Electrical Load Demand Forecasting Using Feed-Forward Neural Networks,” *Energies*, vol. 14, pp. 7644–7667, 2021.
- [34] D.P. Kingma and J. Ba, “Adam: A Method for Stochastic Optimization,” in *3rd International Conference on Learning Representations, ICLR 2015, San Diego, CA, USA, May 7-9, 2015, Conference Track Proceedings*, 2015.
- [35] I. Kaastra and M. Boyd, “Designing a neural network for forecasting financial and economic time series,” *Neurocomputing*, vol. 10, no. 3, pp. 215–236, 1996.
- [36] International Energy Agency (IEA), *Secure Energy Transitions in the Power Sector*, 2021. Available online: <https://www.iea.org/reports/global-energy-review-2021> (accessed on 11 July 2022).